Available online at www.sciencedirect.com

ScienceDirect

Procedia Materials Science 3 (2014) 2122 – 2127

Procedia Materials Science

www.elsevier.com/locate/procedia

20th European Conference on Fracture (ECF20)

Crack paths at multiple-crack systems in anisotropic structures: simulation and experiment

Paul O. Judt[a,*], Andreas Ricoeur[a], Günter Linek[a]

[a]*Department of Engineering Mechanics, Institute of Mechanics, University of Kassel, 34125 Kassel, Germany*

Abstract

This paper is targeted on numerical methods for accurate crack tip loading analysis and crack path prediction. Those are based on finite element calculations of the boundary value problem. Applying path-independent integrals to curved cracks in order to accurately calculate the J-integral, energy release rate (ERR) or stress intensity factors (SIF) is still not state of the art. Contours which are not confined to the crack tip require special analytical preparation and numerical treatment to supply results which are sufficiently precise for reliable crack path prediction. Methods to improve the calculation of the J-integral and the interaction integral (I-integral) are presented. In particular, the latter has never been applied to strongly curved cracks. Also, efficient methods for the loading analysis and crack growth simulation of multiple interacting cracks based on path-independent integrals are presented. The anisotropy of fracture toughness is taken into account being a crucial part of the numerical model. Experiments are carried out with specimens made of aluminum alloy Al-7075, comparing subcritically grown cracks with simulations.

Selection and peer-review under responsibility of the Norwegian University of Science and Technology (NTNU), Department of Structural Engineering

Keywords: crack growth, anisotropy, J-integral, interaction integral, curved cracks

1. Introduction

Predicting the correct crack path in engineering structures is still a cumbersome procedure as many influencing parameters have to be accounted for e.g. crack tip loading, crack deflection criteria, anisotropic and inelastic material behavior. Many researchers of the recent years have focussed on the crack path predictions in plane structures applying different methods and theories and comparing their results to experimental findings (Miranda et al., 2003; Meyer et al., 2006; Španiel et al., 2009). Path-independent integrals are widely applied to calculate loading quantities such as the ERR (Griffith, 1921), SIF (Irwin, 1957), or the J-integral (Rice, 1968).

Budiansky and Rice (1973) extended Rices' approach of J, which was limited to straight cracks, by a formulation of the two-dimensional J_k-integral vector which is composed of the coordinate $J_1 = J$ and J_2. It is well-known that the calculation of the J_2-integral is challenging since the numerical treatment of the singular stresses at the crack tip is going along with problems finally leading to inaccurate results.

* Corresponding author. Tel.: +49-561-804-2852 ; fax: +49-561-804-2720.
E-mail address: judt@uni-kassel.de

Selection and peer-review under responsibility of the Norwegian University of Science and Technology (NTNU), Department of Structural Engineering
doi:10.1016/j.mspro.2014.06.343

The interaction integral is a conservation integral based on the superposition of two loading scenarios (Stern et al., 1976), i.e. the physical (a) and an auxiliary loading (b). In general, the near tip solution is employed to obtain auxiliary fields originally limiting this method to straight cracks in homogeneous materials without interfaces.
After the introduction of path-independent integrals, two new methods for calculating accurate values of J_2 valid for straight and curved cracks are presented. Further, difficulties and solutions are pointed out for the calculation of the I_k-interaction integral considering arbitrary curved crack faces. A second focus is directed at the crack loading analysis of multiple cracks systems. Here, a new procedure is introduced, based on a global I_k-integral calculating accurate loading quantities related to the i-th crack tip by fading out all other crack tips.
Anisotropy in fracture toughness has a strong influence on crack paths and is thus included in the model. A corresponding crack deflection criterion is suggested based on the ERR. Crack paths are calculated and compared to those resulting from experimental findings in rolled Al-7075 plates.

2. Path-independent contour integrals

Within the theory of Linear Elastic Fracture Mechanics (LEFM) the J_k-integral vector is a path-independent energy conservation integral. Applying an integration contour Γ_ϵ in the vicinity of the crack tip at a distance ϵ, the J_k-integral is defined as

$$J_k = \lim_{\epsilon \to 0} \int_{\Gamma_\epsilon} Q_{kj} n_j \mathrm{d}s, \qquad Q_{kj} = \frac{1}{2}\sigma_{mn}\varepsilon_{mn}\delta_{kj} - \sigma_{ij}u_{i,k}, \tag{1}$$

with Eshelby's tensor Q_{kj}, including the stress tensor σ_{mn}, the strain tensor ε_{mn} and the displacement derivatives $u_{i,k}$. The Kronecker identity tensor is denoted as δ_{kj}. In LEFM the coordinates of Eq. (1) are related directly to the SIF:

$$J_1 = \frac{K_\mathrm{I}^2 + K_\mathrm{II}^2}{E'}, \qquad J_2 = -2\,\frac{K_\mathrm{I}\,K_\mathrm{II}}{E'}. \tag{2}$$

For plane stress $E' = E$ and for plane strain $E' = E/\left(1-\nu^2\right)$. If the J_k-integral is calculated, assuming two different superimposed loading scenarios (a) and (b) for an arbitrary crack configuration, one obtains the following expression:

$$J_k^{(\mathrm{a})+(\mathrm{b})} = \lim_{\epsilon \to 0} \int_{\Gamma_\epsilon} Q_{kj}^{(\mathrm{a})+(\mathrm{b})} n_j \mathrm{d}s = \lim_{\epsilon \to 0} \int_{\Gamma_\epsilon} \left(Q_{kj}^{(\mathrm{a})} + Q_{kj}^{(\mathrm{b})} + Q_{kj}^{(\mathrm{a/b})}\right) n_j \mathrm{d}s = J_k^{(\mathrm{a})} + J_k^{(\mathrm{b})} + J_k^{(\mathrm{a/b})}. \tag{3}$$

The third term of Eq. (3) is the interaction integral vector $J_k^{(\mathrm{a/b})}$ and will be denoted from now on as I_k,

$$I_k = \lim_{\epsilon \to 0} \int_{\Gamma_\epsilon} Q_{kj}^{(\mathrm{a/b})} n_j \mathrm{d}s, \qquad Q_{kj}^{(\mathrm{a/b})} = \frac{1}{2}\left(\sigma_{mn}^{(\mathrm{a})}\varepsilon_{mn}^{(\mathrm{b})} + \sigma_{mn}^{(\mathrm{b})}\varepsilon_{mn}^{(\mathrm{a})}\right)\delta_{kj} - \left(\sigma_{ij}^{(\mathrm{a})}u_{i,k}^{(\mathrm{b})} + \sigma_{ij}^{(\mathrm{b})}u_{i,k}^{(\mathrm{a})}\right) \tag{4}$$

with $Q_{kj}^{(\mathrm{a/b})}$ being Eshelby's tensor related to the interaction integral. For straight crack faces, the near-tip solution yields valid fields ε_{mn}, σ_{mn}, $u_{i,k}$ associated to an auxiliary loading configuration and is therefore usually applied as auxiliary field. The relation between the coordinates of Eq. (4) and SIF is as follows:

$$I_1 = 2\,\frac{K_\mathrm{I}^{(\mathrm{a})}K_\mathrm{I}^{(\mathrm{b})} + K_\mathrm{II}^{(\mathrm{a})}K_\mathrm{II}^{(\mathrm{b})}}{E'}, \qquad I_2 = -2\,\frac{K_\mathrm{I}^{(\mathrm{a})}K_\mathrm{II}^{(\mathrm{b})} + K_\mathrm{II}^{(\mathrm{a})}K_\mathrm{I}^{(\mathrm{b})}}{E'}. \tag{5}$$

Auxiliary fields are generally chosen according to an unit mode-I ($K_\mathrm{I}^{(\mathrm{b})} = 1$, $K_\mathrm{II}^{(\mathrm{b})} = 0$) or unit mode-II ($K_\mathrm{I}^{(\mathrm{b})} = 0$, $K_\mathrm{II}^{(\mathrm{b})} = 1$) loading. If finite integration contours Γ_0 are considered, see Fig. 1,the coordinates of J_k and I_k in general become path-dependent (Judt and Ricoeur, 2013b). In case of straight crack faces subjected to mixed-mode loading the path-dependence is restricted to the second coordinates J_2 and I_2 if crack surface loads are neglected. If curved crack faces are considered, both coordinates of J_k and I_k are depending on the chosen integration contour Γ_0. To hold path-independence, crack face integrals have to be introduced, describing the jump of Eshelby's tensor across the physical crack faces $\mathrm{d}\Gamma_\mathrm{c}^+ = -\mathrm{d}\Gamma_\mathrm{c}^- = \mathrm{d}\Gamma_\mathrm{c}$ and the fictitious crack faces $\mathrm{d}\Gamma_\mathrm{f}^+ = -\mathrm{d}\Gamma_\mathrm{f}^- = \mathrm{d}\Gamma_\mathrm{f}$, see Fig. 1(a):

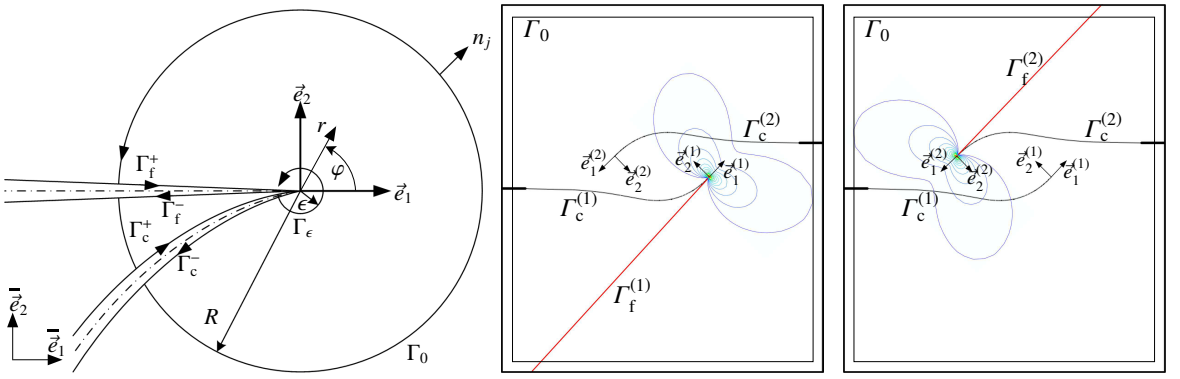

(a) $m = 1$ (b) $m = 1$ (c) $m = 2$

Fig. 1. (a): Integration contours, physical and fictitious crack faces Γ_c and Γ_f for path-independent J_k and I_k-integrals; (b), (c): example of two cracks system and integration contours Γ_0, $\Gamma_c^{(n)}$ and $\Gamma_f^{(m)}$ applied to the calculation of loading quantities.

$$J_k = \int_{\Gamma_0} Q_{kj} n_j \mathrm{d}s + \int_{\Gamma_c} \left[\!\left[Q_{kj} \right]\!\right]_-^+ n_j \mathrm{d}s \tag{6a}$$

$$I_k = \int_{\Gamma_0} Q_{kj}^{(\mathrm{a/b})} n_j \mathrm{d}s + \int_{\Gamma_c} \left[\!\left[Q_{kj}^{(\mathrm{a/b})} \right]\!\right]_-^+ n_j \mathrm{d}s + \int_{\Gamma_F} \left[\!\left[Q_{kj}^{(\mathrm{a/b})} \right]\!\right]_-^+ n_j \mathrm{d}s. \tag{6b}$$

The asymptotic crack tip solutions are selected to be the corresponding auxiliary fields and thus, the fictitious crack faces Γ_f and the physical ones Γ_c always coincide at the crack tip. The integration in the vicinity of the crack tip based on numerical values provided from the FE-calculation is challenging. As the numerical representation of the singularity in stresses and strains deviates strongly from analytic solutions, the calculation of crack face integrals needs a special treatment (Judt and Ricoeur, 2013a) which is usually circumvented applying small contours at the crack tip.

3. Approaches for the accurate calculation of J_2 and I_2

The analytic expression for crack face integrals along a small segment $\mathrm{d}\Gamma_c = \delta$ in the vicinity of the crack tip, where crack faces are approximately straight $\varphi = \pm\pi$ and $n_j = -\vec{e}_2$, is

$$J_k^c = \int_\delta \left[\!\left[Q_{kj} \right]\!\right]_-^+ n_j \mathrm{d}s = 8 \frac{T_{11} K_{II} \sqrt{\delta}}{E' \sqrt{2\pi}} \vec{e}_2 = J_2^c, \qquad I_k^c = \int_\delta \left[\!\left[Q_{kj}^{(\mathrm{a/b})} \right]\!\right]_-^+ n_j \mathrm{d}s = 8 \frac{T_{11}^{(\mathrm{a})} K_{II}^{(\mathrm{b})} \sqrt{\delta}}{E' \sqrt{2\pi}} \vec{e}_2 = I_2^c. \tag{7}$$

The constant T-stress T_{11} at a small distance to the crack tip follows from the representation of tangential normal stress on the crack faces:

$$T_{11} = \frac{1}{2} \left(\sigma_{11}(\delta, +\pi) + \sigma_{11}(\delta, -\pi) \right). \tag{8}$$

Those parts of J_k and I_k which are based on reliable numerical data are calculated from Eqs. (6) where a small part δ at the crack faces is excluded. The remaining part of the integrals is expressed analytically by Eqs. (7). Here, the analytic part I_k^c is directly calculated applying T_{11} according to Eq. (8). In contrast, J_k^c is evaluated by an iterative procedure, as the analytic integral depends on the values of J_k. This becomes obvious, as the unknown value K_{II} is calculated from the coordinates J_k by rearranging Eqs. (2).

A second approach for the accurate calculation of J_k^c is the extrapolation of tangential normal stresses and strains on the crack faces. The crack face integral incorporates the jump of the strain energy density across the positive and

negative crack faces $[\![u]\!]^{+}_{-}$, with $u = (\sigma_{11}\varepsilon_{11})/2$. Investigations show that values of tangential normal stresses σ_{11} and strains ε_{11} on the crack faces related to a mode-I loading should reach a constant value at the crack tip. In contrast, values related to a mode-II loading are singular there. Numerically calculated values of σ_{11} and ε_{11}, respectively, become highly inaccurate approaching the crack tip. The values related to the single mode cases are separated as follows:

$$\sigma_{11}^{\mathrm{I}} = \frac{1}{2}\left(\sigma_{11}^{\Gamma_C^+} + \sigma_{11}^{\Gamma_C^-}\right), \qquad \sigma_{11}^{\mathrm{II}\pm} = \sigma_{11}^{\Gamma_C^\pm} - \sigma_{11}^{\mathrm{I}}, \qquad \varepsilon_{11}^{\mathrm{I}} = \frac{1}{2}\left(\varepsilon_{11}^{\Gamma_C^+} + \varepsilon_{11}^{\Gamma_C^-}\right), \qquad \varepsilon_{11}^{\mathrm{II}\pm} = \varepsilon_{11}^{\Gamma_C^\pm} - \varepsilon_{11}^{\mathrm{I}}. \tag{9}$$

Mode-I values σ_{11}^{I} and $\varepsilon_{11}^{\mathrm{I}}$ within the region $[0, \delta]$ are replaced by those calculated from a linear regression based on values at $r > \delta$. The integral is calculated classically according to Eq. (6a) considering the extrapolated values.

4. Global approach for crack tip loading analyses in multiple cracks systems

In LEFM the ERR $G^{(n)}$ of a crack n equals the projection of the J_k-integral vector onto the unit vector of crack propagation z_k:

$$-\frac{1}{B}\frac{\mathrm{d}\Pi}{\mathrm{d}a^{(n)}} = G^{(n)} = J_k^{(n)} z_k^{(n)}. \tag{10}$$

The width B of the specimen will be dropped from now on whereupon the ERR has the unit J/m and must be divided by B to obtain the physical quantity. The virtual change of the total potential energy equals the product of the ERR and the virtual crack extension δa:

$$\delta\Pi = \frac{\mathrm{d}\Pi}{\mathrm{d}a}\delta a = -G\delta a. \tag{11}$$

Taking into account that $\delta a^{(n)} = \delta a$ for all crack tips, the change of potential energy of a system with N cracks reads

$$\delta\Pi = -\sum_{n=1}^{N} G^{(n)}\delta a^{(n)} = -\sum_{n=1}^{N} G^{(n)}\delta a. \tag{12}$$

It becomes clear from Eq. (12), that the total energy release of a system with N cracks is the sum of individual ERRs for each single crack n, according to

$$\tilde{G} = -\frac{\mathrm{d}\Pi}{\mathrm{d}a} = \sum_{n=1}^{N} G^{(n)} = \sum_{n=1}^{N} J_k^{(n)} z_k^{(n)} \tag{13}$$

where $\tilde{G}$ is a global ERR. Within a local crack tip coordinate system $\vec{e}_k^{\,(n)}$ related to the n-th crack, see Figs. 1(b) and 1(c), the first coordinate $J_1^{(n)}$ is related to the ERR $G^{(n)}$ in case of a self-similar crack propagation $z_k^{(n)} = \vec{e}_1^{\,(n)}$. Consistent with Eq. (13) and considering Eq. (5) the interaction integral of multiple cracks systems equals the sum of the interaction integrals related to each crack tip:

$$\tilde{G}^{(\mathrm{a/b})} = \tilde{I}_1 = \sum_{n=1}^{N} I_1^{(n)} = \frac{2}{E'}\sum_{n=1}^{N}\left[{}^{(\mathrm{a})}K_{\mathrm{I}}^{(n)}\,{}^{(\mathrm{b})}K_{\mathrm{I}}^{(n)} + {}^{(\mathrm{a})}K_{\mathrm{II}}^{(n)}\,{}^{(\mathrm{b})}K_{\mathrm{II}}^{(n)}\right]. \tag{14}$$

A global interaction integral approach according to Eq. (14) basically has to deal with interacting auxiliary fields and thus additional terms in Eq. (4). The integration path Γ_0 is including all crack tips, thus the approach is denoted as "global". In Eq. (14) $2N$ SIF of the physical problem are unknown. To determine these values, the choice of SIF related to the auxiliary fields is similar as explained in Sec. 2 for the single-crack problem. Now, all SIF of the auxiliary fields ${}^{(\mathrm{b})}K_{\mathrm{I/II}}$ are chosen to be zero except for the m-th crack. In this case, the global interaction integral according to Eq. (14) simplifies and for auxiliary unit mode-I (superscript I) and unit mode-II loadings (superscript II) reads:

$$\tilde{I}_1^{\mathrm{I}} = I_1^{(m)} = \frac{2}{E'}{}^{(\mathrm{a})}K_{\mathrm{I}}^{(m)}, \qquad \tilde{I}_1^{\mathrm{II}} = I_1^{(m)} = \frac{2}{E'}{}^{(\mathrm{a})}K_{\mathrm{II}}^{(m)}. \tag{15}$$

This choice equals the procedure of defining only one auxiliary field related to the m-th crack tip. Thus, the interaction of multiple auxiliary fields and therefore additional terms in the I_k-integral calculation according to Eq. (4) is prevented as these terms are canceled out. Now that all cracks except one are faded out, the integration contour may be chosen on a global level, i.e. all crack tips are included. The integration contours chosen for this global approach, are exemplarily shown in Figs. 1(b) and 1(c) for a system with $N = 2$ cracks. The general formulation of the path invariant I_k-integral thus considers integrations along the external contour Γ_0 and along all N physical and fictitious crack faces, $\Gamma_\mathrm{c}^{(n)}$ and $\Gamma_\mathrm{f}^{(n)}$. As the auxiliary fields are inserted according to the above discussed choice of the auxiliary SIF, according to which all are zero except for the m-th crack, the I_k-integral simplifies as follows:

$$I_k^{(m)} = \int_{\Gamma_0} Q_{kj}^{(\mathrm{a/b})} n_j \mathrm{d}s + \sum_{n=1}^{N} \int_{\Gamma_\mathrm{c}^{(n)}} \left[\!\left[Q_{kj}^{(\mathrm{a/b})} \right]\!\right]_-^+ n_j \mathrm{d}s + \int_{\Gamma_\mathrm{f}^{(m)}} \left[\!\left[Q_{kj}^{(\mathrm{a/b})} \right]\!\right]_-^+ n_j \mathrm{d}s. \tag{16}$$

5. Comparison of experimental and numerical crack paths

The concepts presented in the previous sections are applied to accurate crack path predictions. The J_k- and I_k-integrals are implemented as post processors into the commercial FE code ABAQUS. The simulation of stable and subcritical crack growth is realized by an incremental extensions of the crack faces. In the past, many crack deflection criteria were presented e.g. by Erdogan and Sih (1963) or Hussain et al. (1974). The deviation of crack paths derived from different deflection criteria is negligible for small mixed-mode ratios $|K_\mathrm{II}/K_\mathrm{I}| < 0.1$.
The J-integral criterion assumes that the crack always grows in the direction of the J_k-vector, as the ERR is maximized in that case. According to Eq. (10) the ERR can be expressed as a quantity depending on the crack deflection angle α

$$G(\alpha) = J_1 \cos\alpha + J_2 \sin\alpha. \tag{17}$$

Most fracture criteria assume isotropic critical parameters K_Ic or G_c which are independent of the crack growth direction. G_c is related to the fracture toughness K_Ic by

$$G_\mathrm{c} = \frac{K_\mathrm{Ic}^2}{E}. \tag{18}$$

Due to rolling process during production, plates of Al-7075 show anisotropic effects in fracture toughness which must be considered in the modeling and prediction of crack growth. In general, the fracture toughness in rolling direction (RD) K_Ic^{RD} is smaller than in transversal direction (TD) K_Ic^{TD}. Kfouri (1996) presented an elliptical interpolation function describing the fracture toughness as a function of the orientation angle α with respect to the RD:

$$\left(\frac{1}{K_\mathrm{c}(\alpha)}\right)^2 = \left(\frac{\cos\alpha}{K_\mathrm{c}^\mathrm{RD}}\right)^2 + \left(\frac{\sin\alpha}{K_\mathrm{c}^\mathrm{TD}}\right)^2, \qquad \frac{1}{G_\mathrm{c}(\alpha)} = \frac{\cos^2\alpha}{G_\mathrm{c}^\mathrm{RD}} + \frac{\sin^2\alpha}{G_\mathrm{c}^\mathrm{TD}}. \tag{19}$$

Besides $G_\mathrm{c}(\alpha)$ the loading quantity $G(\alpha)$ depends on the crack deflection angle. On the one hand, the system attempts to minimize the total potential energy and therefore maximize the energy release rate during the crack advance $G(\alpha) \stackrel{!}{=} \max$. On the other hand, the crack tends to grow into the direction of the minimum material resistance $G_\mathrm{c}(\alpha) \stackrel{!}{=} \min$. The ratio of ERR and crack resistance according to Eqs. (17) and (19) is defined as

$$G_\mathrm{R}(\alpha) = \frac{G(\alpha)}{G_\mathrm{c}(\alpha)} = \frac{J_1 \cos^3\alpha + J_2 \sin\alpha\, \cos^2\alpha}{G_\mathrm{c}^\mathrm{RD}} + \frac{J_1 \cos\alpha\, \sin^2\alpha + J_2 \sin^3\alpha}{G_\mathrm{c}^\mathrm{TD}}. \tag{20}$$

It is assumed, that the crack grows in the direction of maximum G_R, thus $\partial G_\mathrm{R}/\partial\alpha = 0$ and $\partial^2 G_\mathrm{R}/\partial\alpha^2 < 0$. Numerically predicted crack paths for different ratios of anisotropy $\chi = K_\mathrm{Ic}^{TD}/K_\mathrm{Ic}^{RD}$ are presented in Fig. 2 and compared with experiments. Experiments with CT specimens were carried out for rolled Al-7075 providing a ratio of $\chi = 1.14$. Comparing crack paths in Fig. 2(a) it is obvious that the anisotropy of fracture toughness is crucial for crack path prediction although the ratio $\chi = 1.14$ slightly overestimates the crack deflection by the hole.

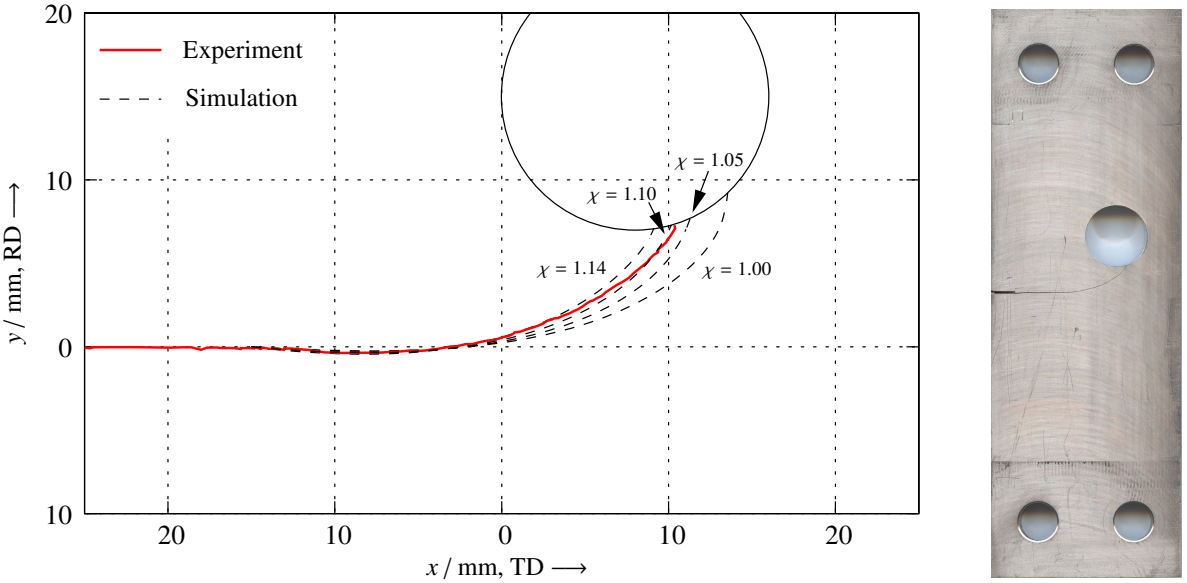

(a) Experimentally and numerically determined crack paths (b) Specimen with crack

Fig. 2. Comparison of crack growth experiment and simulations for plate of Al-7075

6. Closure

New approaches have been presented for the accurate calculation of crack face contribution to J_k- and I_k-integrals enabling the application of remote integration contours. This leads to efficient simulations of crack problems considering internal boundaries or multiple crack faces. A new method for the separation of loading quantities at multiple cracks systems based on global I_k-integrals is presented. It is shown that the fracture toughness anisotropy has a strong impact on crack paths and must be considered in numerical models. Experiment and prediction are in good agreement.

References

Budiansky, B., Rice, J., 1973. Conservation laws and energy-release rates. Journal of Applied Mechanics 40, 201–203.

Erdogan, F., Sih, G., 1963. On the crack extension in plates under plane loading and transverse shear. Journal of Basic Engineering 85, 519–527.

Griffith, A., 1921. The phenomena of rupture and flow in solids. Philosophical Transactions of the Royal Society of London, Series A 221, 163–198.

Hussain, M., Pu, S., Underwood, J., 1974. Strain energy release rate for a crack under combined mode I and mode II. Fracture Analysis, ASTM STP 560 , 2–28.

Irwin, G., 1957. Analysis of stresses and strains near the end of a crack traversing a plate. Journal of Applied Mechanics 24, 361–364.

Judt, P., Ricoeur, A., 2013a. Accurate loading analyses of curved cracks under mixed-mode conditions applying the J-integral. International Journal of Fracture 182, 53–66.

Judt, P., Ricoeur, A., 2013b. Efficient simulation of crack growth in multiple-crack systems considering internal boundaries and interfaces, in: Advances in Fracture Research, Proceedings of the ICF13.

Kfouri, A., 1996. Crack extension under mixed-mode loading in an anisotropic mode-asymmetric material in respect of resistance to fracture. Fatigue and Fracture of Engineering Materials and Structures 19, 27–38.

Meyer, A., Rabold, F., Scherzer, M., 2006. Efficient finite element simulation of crack propagation using adaptive iterative solvers. Communications in Numerical Methods in Engineering 22, 93–108.

Miranda, A., Meggiolaro, M., Castro, J., Martha, L., Bittencourt, T., 2003. Fatigue life and crack path predictions in generic 2D structural components. Engineering Fracture Mechanics 70, 1259–1279.

Rice, J., 1968. A path independent integral and the approximate analysis of strain concentration by notches and cracks. Journal of Applied Mechanics 35, 379–386.

Stern, M., Becker, E., Dunham, R., 1976. A contour integral computation of mixed-mode stress intensity factors. International Journal of Fracture 12, 359–368.

Španiel, M., Jurenka, J., Kuželka, J., 2009. Verification of fe model of fatigue crack propagation under mixed mode conditions. Meccanica 44, 189–195.